MICROBIOLOGY

RESEARCH ARTICLE

Nazik *et al.*, *Microbiology* 2017;163:1568–1577

DOI 10.1099/mic.0.000539

MICROBIOLOGY SOCIETY

Pseudomonas phage inhibition of *Candida albicans*

Hasan Nazik,[1,2,*] Lydia-Marie Joubert,[3] Patrick R. Secor,[4] Johanna M. Sweere,[2,5] Paul L. Bollyky,[2,5] Gabriele Sass,[1,2] Lynette Cegelski[6] and David A. Stevens[1,2]

Abstract

Pseudomonas aeruginosa (Pa) and *Candida albicans* (Ca) are major bacterial and fungal pathogens in immunocompromised hosts, and notably in the airways of cystic fibrosis patients. The bacteriophages of Pa physically alter biofilms, and were recently shown to inhibit the biofilms of *Aspergillus fumigatus*. To understand the range of this viral–fungal interaction, we studied Pa phages Pf4 and Pf1, and their interactions with Ca biofilm formation and preformed Ca biofilm. Both forms of Ca biofilm development, as well as planktonic Ca growth, were inhibited by either phage. The inhibition of biofilm was reversed by the addition of iron, suggesting that the mechanism of phage action on Ca involves denial of iron. Birefringence studies on added phage showed an ordered structure of binding to Ca. Electron microscopic observations indicated phage aggregation in the biofilm extracellular matrix. Bacteriophage–fungal interactions may be a general feature with several pathogens in the fungal kingdom.

INTRODUCTION

Pseudomonas aeruginosa (Pa) is the principal bacterial pathogen in cystic fibrosis (CF) airways [1], while *Aspergillus fumigatus* (Af) and *Candida albicans* (Ca) are the principal fungal pathogens [2–6], and these are the principal pathogens in other immunocompromised patients, particularly neutropenic patients. Thus the interactions of these bacterial–fungal pathogen pairs, which are relevant to their coexistence in the human body, particularly CF airways, have been of considerable interest. All three of these pathogens form biofilms *in vitro* and *in vivo*, which will affect their interactions. Several studies have illuminated the molecular species that may be involved in the interactions of Pa–Af (reviewed in [7]) and Pa–Ca [8–15].

Phages, viruses that infect Pa and other bacteria, have been of interest to us. We showed that phages from Pa can – extremely rapidly – affect the physical structures of a biofilm (Pa) [16]. Subsequently, we reported the also novel finding that Pa phages could not only affect the structure of a *fungal* (Af) biofilm, but also inhibit fungal metabolism and growth, and do that by denying iron (Fe) to the fungus [17]. It was thus of interest whether this phage–fungus interaction was unique to Af, or whether the findings could apply more broadly to other fungal pathogens. We therefore present here studies of inovirus phages with Ca, a fungal pathogen whose chronic colonization of CF airways has been shown [18], and which is associated in some studies with deterioration of CF lung function [19, 20].

METHODS

C. albicans and growth conditions

C. albicans 5 (Ca5), a virulent clinical isolate [21], was used throughout this study. Ca5 was taken from stock suspensions stored at −80 °C and then grown overnight on Sabouraud dextrose agar (Beckton Dickinson and Co., Sparks, MD, USA) at 37 °C.

A loopful of the yeasts was inoculated in 10 ml RPMI-1640 (Lonza, Walkersville, MD, USA) in loosely capped 50 ml centrifuge tubes. After overnight culturing of the broth at 37 °C (65–70 r.p.m. shaking conditions), the cells were harvested by centrifugation (2000 ***g*** for 5 min) and the supernatant was removed. The pellet was washed twice by resuspension in 20 ml of phosphate-buffered saline (PBS), vortex mixing and then re-centrifugation.

The final pellet of cells was resuspended in 10 ml of RPMI-1640 and a cell suspension and 1 : 100 or 1 : 1000-fold

Received 6 August 2017; Accepted 15 September 2017

Author affiliations: [1]California Institute for Medical Research, San Jose, CA, USA; [2]Division of Infectious Diseases, Department of Medicine, Stanford University Medical School, Stanford, CA, USA; [3]Cell Sciences Imaging Facility, Stanford University Medical School, Stanford, CA, USA; [4]Division of Biological Sciences, University of Montana, Missoula, MT, USA; [5]Immunology Program, Stanford University, Stanford, CA, USA; [6]Department of Chemistry, Stanford University, Stanford, CA, USA.

***Correspondence:** Hasan Nazik, hasannazik01@gmail.com

Keywords: *Candida albicans*; *Pseudomonas aeruginosa*; bacteriophage; biofilm; iron.

Abbreviations: CF, cystic fibrosis; CPD, critical-point-dried; HMDS, hexamethyldisilazane; LB, lysogeny broth; TIFF, tagged image file format; XTT, 2,3-bis[2-methoxy-4-nitro-5-sulfophenyl]-2H-tetrazolium-5-carboxanilide inner salt.

dilutions in the same medium prepared and counted using a hemocytometer and bright field microscope with a 40× objective.

In vitro model of biofilm development

The *Candida* biofilm methodology was derived from previous publications [22–26]. Flat-bottom 96-well culture plates (Corning Inc., Corning, NY, USA) containing a final volume of 200 µl were used for biofilm development. The final cell concentration in each well was 5×10^5 yeast cell ml^{-1}. The plates were incubated at 37 °C for 16 h with shaking at 65–70 r.p.m. to allow the yeast cells to attach to the surface. Following the biofilm formation phase, the wells were rinsed twice gently in sterile 200 µl PBS $well^{-1}$, fresh RPMI-1640 was put in the wells and then they were incubated for an additional 24 h at 37 °C with shaking at 65–70 r.p.m.

Phage preparation

Two phages from Pa (Pf1, Pf4) were studied. Pa strain K (PAK, ATCC 25102) produced Pf1 (ATCC 25102B) and Pa strain PAO1 produced Pf4. In particular, we used strain MPAO1, originating from the laboratory of Dr Colin Manoil [27], which only carries the Pf4 prophage and not RPG42. Phages were harvested as described previously [28]. In brief, bacteria were cultured in a 250 ml volume lysogeny broth (LB) (Sigma, St Louis, MO, USA) for 48 h at 37 °C under shaking conditions. Bacteria were removed by centrifugation and the supernatant was sterilized by vacuum filtration through a 0.22 µm filter. Crude supernatant was treated with 1 µg ml^{-1} DNase (Sigma) for 2 h at 37 °C. Phages were precipitated from the supernatant by adding 0.5M NaCl and 4 % polyethylene glycol (PEG) 8000 (Sigma) and incubating the phages overnight at 4 °C. Phages were then pelleted by centrifugation, washed in sterile buffer and subjected to another round of PEG precipitation. Finally, the purified phages were suspended in sterile PBS and dialyzed in a 50 kDa cut-off dialysis tube (Spectrum Laboratories, Rancho Dominguez, CA, USA) against PBS. Stocks of approximately 10^{13} phage ml^{-1} were thus produced.

Quantitation of Pf phage

Purified Pf phage was quantified by *Taq*man PCR amplification of a 52-bp region in the PA0717 gene, which codes for a hypothetical protein and is conserved across the Pf1, Pf4 and Pf5 phages. Purified Pf phage preparations were treated with 1 µg ml^{-1} DNase I (Roche, Indianapolis, IN, USA) at 37 °C for 1 h to remove potential contaminating Pa DNA. Samples were then boiled at 100 °C for 10 min in a Bio-Rad (Hercules, CA, USA) T100 thermo cycler, removing the DNase and releasing the protected phage DNA. One µl of the template was added to a master mix of 5 µl 2× SensiFAST Probe Hi-Rox Mix (Bioline, London, UK); 1 µl forward primer (TTCCCGCGTGGAATGC, stock concentration 6 µM); 1 µl reverse primer (CGGGAAGACAGCCACCAA, stock concentration 4 µM); 2 µl labelled probe (AACGCTGGGTCGAAG, stock concentration 1 µM); and 1 µl ultrapure water (10 µl total). In order to calculate the Pf phage concentration per reaction, the assay included a standard made from a pUC57 plasmid containing the PA0717 amplification sequence. The PCR was run on an Applied Biosystems (Waltham, MA, USA) StepOne Plus machine using a specialized *Taq*man program [(95 °C 2 min, (95 °C 15 s, 60 °C 20 s) × 40 cycles].

A 'mock phage' preparation was processed from media through all the steps used for the phage preparations, as a negative control. A second negative control was processed identically from a phage-deficient *Pa* mutant. This strain, PAO1 Δ*PA0728,* was created by allelic exchange [29] using the deletion construct pEX-ΔPA0728 [30] as described [16]. PAO1 Δ*PA0728,* is derived from strain PAO1 but lacks the phage integrase gene (*PA0728*) and is not able to maintain the replicative form of Pf4 [30]. The deletion of *PA0728* was confirmed by sequencing [17]. Neither of these controls showed activity in any of the assays that are described in the Results section.

Direct effect of bacteriophage on *C. albicans* biofilm formation

Ten-fold dilutions of Pf1 or Pf4 phage in RPMI-1640 were made, and added (in one-tenth the volume) to the biofilm media at the start of the biofilm formation phase. The data are expressed in terms of the final phage concentration/ml. Plates were incubated at 37 °C for 16 h with shaking at 65–70 r.p.m. The wells then were rinsed twice gently in 200 µl sterile PBS per well before fresh RPMI-1640 was put into each well, with these being incubated for an additional 24 h at 37 °C with shaking at 65–70 r.p.m.

The effects were evaluated by XTT assay. The tetrazolium salt, XTT (2,3-bis[2-methoxy-4-nitro-5-sulfophenyl]−2H-tetrazolium-5-carboxanilide inner salt) (Sigma), was used to measure the metabolic activity of Ca. The wells, as described above, were rinsed twice in sterile PBS, 200 µl sterile PBS containing 200 µg ml^{-1} XTT and 40 µM menadione (Sigma) was added, and the plates were incubated in the dark for 2 h at 37 °C without shaking. Following incubation, the plates were centrifuged for 5 min at 2000 ***g*** and 100 µl supernatant from each well was transferred into sterile 96-well plates for reading at 490A with a microtitre plate reader (Dynex Technologies, Inc., Chantilly, VA, USA).

Direct effect of bacteriophage on preformed *C. albicans* biofilm

Ca biofilms were formed as described above. After 16 h, the wells containing the preformed biofilms were washed gently in sterile PBS and fresh phage dilutions in RPMI-1640 were added, as described above. The plates were incubated for an additional 24 h at 37 °C with shaking at 65–70 r.p.m. The effects were evaluated by the XTT assay.

We also performed these phage studies – with both biofilm formation and preformed biofilm – under hypoxic conditions using the Gas-Pak EZ Campy Pouch system (Becton Dickinson) (as previously detailed) [31], and compared the results to those for the aerobic conditions that form the basis of the present communication.

To assess whether any differences could be seen with respect to the interactions with phage in the larger volumes that would be required for the electron microscopy studies (to be described), assays were also performed in the 8-well and 12-well formats previously described [32]. As no differences were noted between the 8-, 12- and 96-well formats, these results are considered together in the Results section.

Reversal of Pf1/Pf4 inhibition of *C. albicans* biofilm formation and preformed biofilm with $FeCl_3$

To examine whether phage inhibition of Ca biofilm formation is related to Ca iron metabolism, the activity of Pf1 or Pf4 against Ca biofilm formation, or preformed biofilm, prepared as described above, was tested in the presence of dilutions of $FeCl_3$ (Sigma). Briefly, $FeCl_3$ was diluted to varying concentrations in RPMI-1640 and distributed in 100 µl quantities in selected wells.

We found that in the experiments where exogenous iron was added, the XTT results were erratic, unless the XTT mixture was removed from the wells after the XTT incubation step, with the wells being washed once with PBS, before the biofilm was studied at 490A.

Culture of *C. albicans* biofilms for birefringence measurements

Ca, strain Ca5 cell suspensions were prepared as described above. The suspension was diluted further to 10^6 cell ml^{-1} as the working suspension. Sixteen-well sterile chamber slides with covers (Thermo Fisher Scientific, Waltham, MA, USA) were used for the development of Ca biofilm. A suspension of Ca (100 µl) was placed into each well with 100 µl fresh RPMI-1640. The chamber slides were incubated for 16 h at 37 °C at 65–70 r.p.m on a shaker to allow the yeast to form biofilm. After 16 h of biofilm formation, verified microscopically, the medium was aspirated and the wells were washed gently twice with 200 µl sterile PBS. After the addition of 200 µl of fresh RPMI-1640 to each well, the slides were incubated for an additional 22 h at 37 °C at 65–70 r.p.m on a shaker. After a total of 38 h of incubation, the medium in the wells was replaced with fresh RPMI-1640 with or without Pf1 or Pf4 phage (10^{10} phage ml^{-1}). Ca biofilm with RPMI-1640 without phage served as a control. After an additional 2 h incubation at 37 °C at 65–70 r.p.m., the medium was aspirated from each well and 100 µl paraformaldehyde (4 % w/v) (Sigma) was put into each well. The slides were held at room temperature overnight. The paraformaldehyde in the wells was replaced with 100 µl distilled water.

Statistical analysis

Each study performed in the wells included six replicates. The data from the experiments using XTT assay were analysed using a *t* test. All statistical analyses were performed using GraphPad Prism (GraphPad Software, San Diego, CA, USA). Statistical significance was considered as $P<0.05$.

Metabolic MIC assay

Ca strain Ca5 yeasts (10^6) were prepared in a volume of 900 µl RPMI. Ten-fold dilutions of Pf1 or Pf4 were prepared in a volume of 100 µl PBS, and added to the yeast preparations. Instead of phage dilutions, 100 µl PBS served as a negative control. Following incubation at 37 °C for 48 h, with shaking at 100 r.p.m., an XTT assay was performed on the planktonic growth to measure Ca5 metabolic activity. Briefly, 1 ml XTT (300 µg ml^{-1}) and 1.5 µl menadione (100 mM) were added to each MIC reaction and incubated at 37 °C for 30 min. The tubes were centrifuged and supernatants were measured at 490 nm using a spectrophotometer (Genesys 20, Thermo Fisher Scientific, Inc).

Birefringence measurements

The birefringence of Ca biofilms grown with and without phage was measured using the Rotopol imaging system [33], as previously described [17]. Briefly, samples were placed in-between a rotating polarizer and circular analyser and imaged. The images were analysed using Rotopol software and the birefringence was computed as $|\sin\delta|$. The mean values of $|\sin\delta|$ were measured in areas in the focal plane with no obstructions in the background.

Scanning electron microscopy (SEM)

Pf1 or Pf4 phage or diluent (control) were added at the initiation of the *Candida* cultures, or at 16 h after initial biofilm formation, or after 38 h, when there had been some incubation time in the initial biofilm state. Preparations for microscopy were made at 40 h. For SEM analysis, samples were immersed in Tris buffer, fixed for 45 min with 4 % paraformaldehyde and 2 % glutaraldehyde in 0.1M sodium cacodylate buffer (pH 7.4), rinsed in the same buffer and post-fixed for 45 min with 1 % aqueous OsO_4. After dehydration in an ascending ethanol series [50, 70, 90, 100 % (twice); 5 min each], the samples were either critical-point-dried (CPD) with liquid CO_2 in a Tousimis Autosamdri-815B apparatus (Tousimis, Rockville, MD, USA) or – where the glass multiwell slides exceeded the CPD chamber size – treated with hexamethyldisilazane (HMDS) for 30 min before overnight drying in a desiccator. The slide chambers were gently removed from the glass substrate before the substrates were mounted onto 15–50 mm circular aluminium stubs (Electron Microscopy Sciences, Hatfield, PA, USA) and sputter-coated with 50 Å of gold/palladium using a Denton Desk II sputter coater (Denton Vacuum, Moorestown, NJ, USA). Visualization was performed with a Zeiss Sigma FESEM (Carl Zeiss Microscopy, Thornwood, NY, USA) operated at 2-4kV, using InLens secondary electron detection at a working distance of 4–5 mm. The images were captured in TIFF using the store resolution of 2048×1536 and a line averaging noise reduction algorithm.

RESULTS

Effect of Pf4 phage on *Candida* biofilm formation

When the Pf4 phage was studied in the same manner as in previous *Aspergillus* studies [17], i.e. being added to Ca at

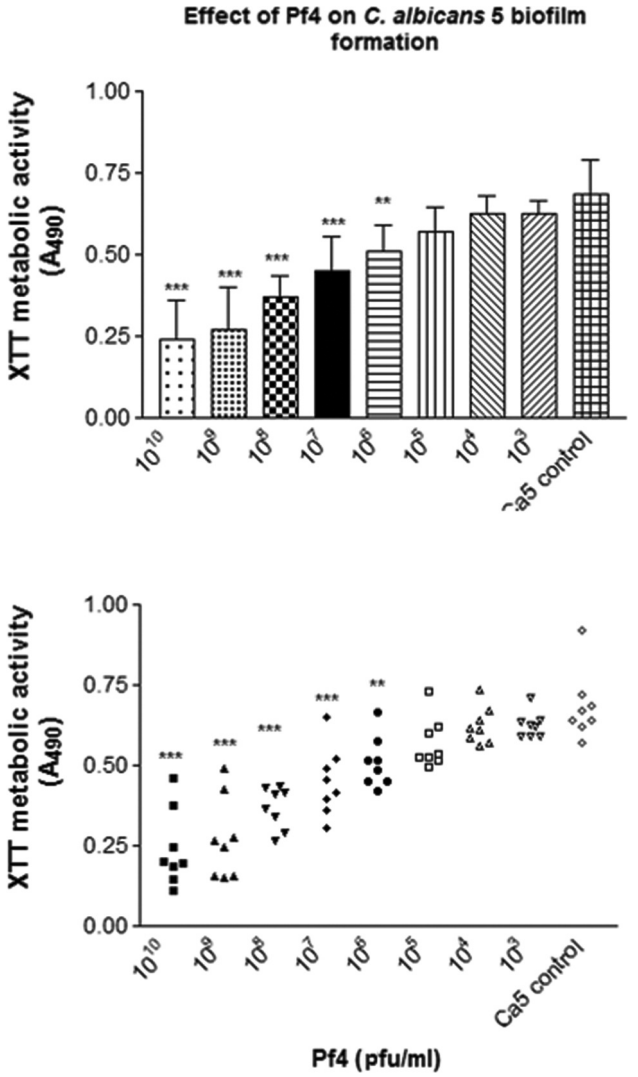

Fig. 1. Effect of Pf4 on *C. albicans* biofilm formation. XTT results for *C. albicans,* strain 5, treated with Pf4 phage, compared to the results for the untreated control ('Ca5 control'). The quantity of phage added is shown on the *x*-axis (the phage concentrations in figures are expressed as final concentrations/ml of culture). Bottom: scattergram showing the distribution of replicate wells. Two and three asterisks represent $P \leq 0.01$ and $P \leq 0.001$, respectively, compared to the untreated control.

the outset of biofilm formation, the metabolism of Ca was inhibited in a dose-responsive manner at the end of the study period. Fig. 1 is representative of 10 experiments. When studying 10-fold dilutions, significant ($P \leq 0.05$) inhibition occurred with dilutions from 10^{10} to 10^{6} phage ml^{-1}. This figure is also displayed to show the results for individual replicate wells (bottom half), which are representative of how the data were derived for the means and standard deviations shown in the top half of the figure, as well as subsequent figures, where only the aggregate data are shown (because of space considerations).

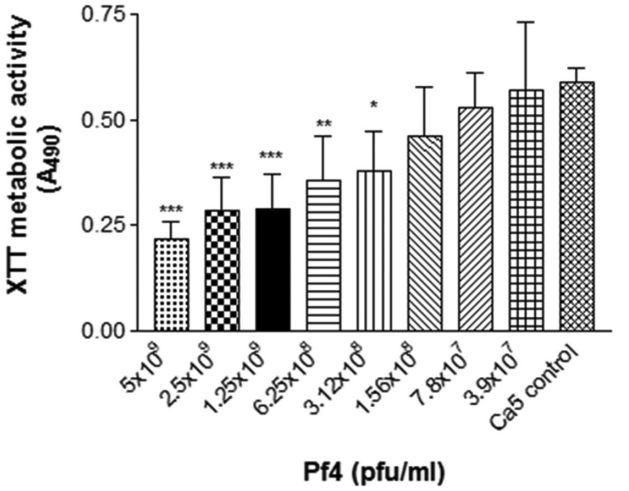

Fig. 2. Effect of Pf4 on preformed *C. albicans* biofilm. XTT results for *C. albicans* treated with Pf4 phage compared to that left untreated ('Ca5 control'). The quantity of phage added is on the *x*-axis, as in Fig. 1. One, two and three asterisks are $P \leq 0.05$, $P \leq 0.01$ and $P \leq 0.001$, respectively, compared to the untreated control.

Effect of Pf4 on preformed *C. albicans* biofilm

The Pf4 phage was studied similarly after the formation of biofilm through incubation with preformed biofilm. Inhibition of biofilm XTT in preliminary studies using 10-fold dilutions was noted at 10^{9} phage ml^{-1}. To refine the cutoff for significant activity, twofold dilution series were made. Fig. 2 is representative of 11 experiments. These showed significant inhibitory activity to a dilution of 3×10^{8}

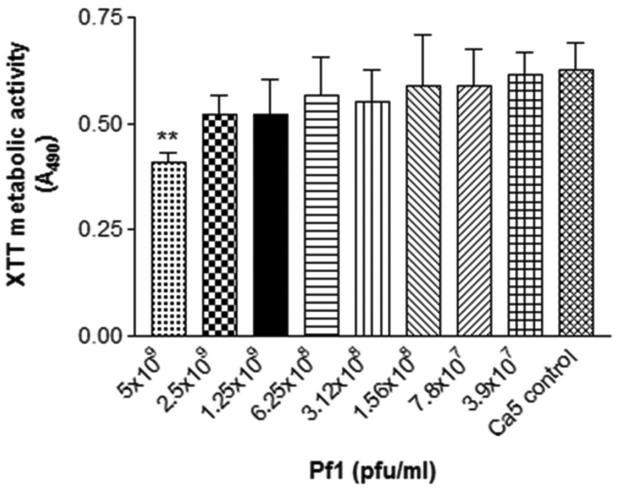

Fig. 3. Effect of Pf1 on *C. albicans* biofilm formation. XTT results for *C. albicans* treated with Pf1 phage compared to that left untreated ('Ca5 control'). The quantity of phage added is on the *x*-axis, as in Figs 1 and 2. Two asterisks, $P \leq 0.01$ compared to untreated control.

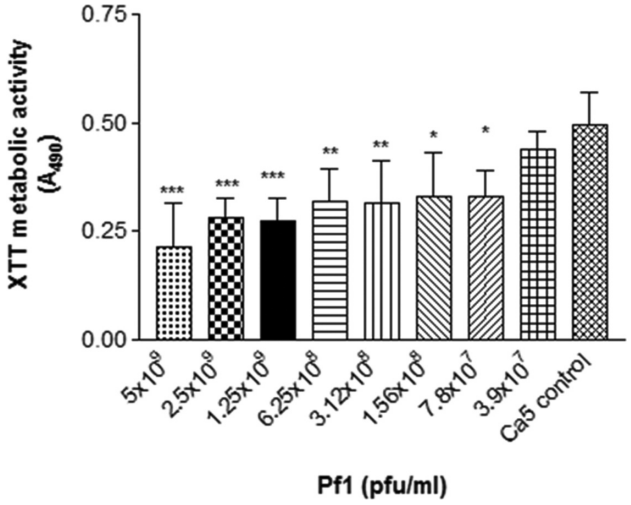

Fig. 4. XTT results for *C. albicans* preformed biofilm treated with Pf1 phage compared to that left untreated ('Ca5 control'). The quantity of phage added is on the *x*-axis, as in Figs 1, 2 and 3. One, two and three asterisks indicate $P \leq 0.05$, $P \leq 0.01$ and $P \leq 0.001$, respectively, compared to the untreated control.

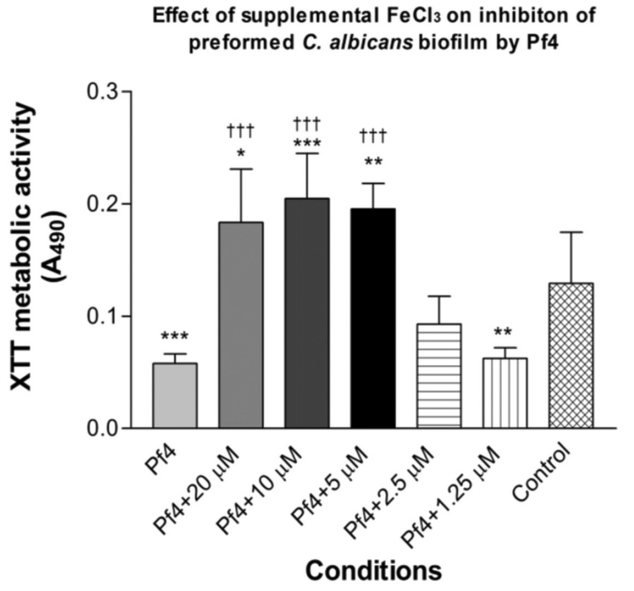

Fig. 6. Reversal by Fe of Pf4 inhibition of preformed *C. albicans* biofilm (XTT assay). 'Control' is no Fe or phage. Pf4 in all other bars was 10^{10} pfu/ml. Fe at 5–20 µM eliminates the Pf4 inhibition, at 2.5 µM it neutralizes the Pf4 effect without enhancement of XTT and at 1.25 µM it has no reversal effect. In this experiment Pf4+0.625, 0.312 or 0.156 µM Fe were also studied (not shown), with those three combinations not differing from Pf4+1.25 µM. One, two and three asterisks indicate $P \leq 0.05$, $P \leq 0.01$ and $P \leq 0.001$, respectively, compared to the untreated control. Three daggers, $P \leq 0.001$, compared to Pf4 alone.

phage ml^{-1}, with approximately 100-fold less activity against biofilm formation.

Effect of Pf1 phage on *C. albicans* biofilm formation

The biofilm formation studies were repeated with Pf1 phage. Inhibition of biofilm XTT in preliminary studies was noted at 10^{10} phage ml^{-1}. To refine the cutoff for significant activity, twofold dilution series were again made. Fig. 3 is representative of 10 experiments. The lowest dilution showing significant activity was 5×10^9 phage ml^{-1}, showing approximately 1000–10 000-fold less activity than the Pf4 phage against biofilm formation.

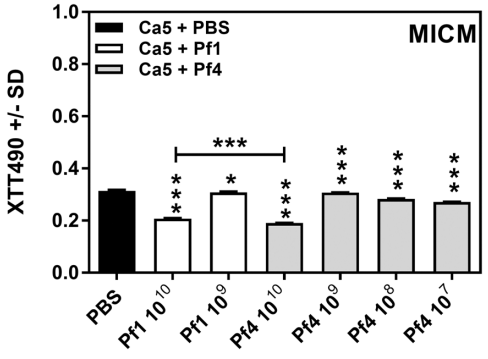

Fig. 5. MIC determination for Ca5 planktonic growth with XTT metabolic assessment. The quantity of phage added is on the *x*-axis. Pf1 dilutions, white bars; Pf4 dilutions, grey bars. The horizontal bar compares Pf4 inhibition with lesser Pf1 inhibition. The vertical asterisks compare bars with control (PBS, black bar). One and three asterisks indicate $P \leq 0.05$ and $P \leq 0.001$ comparisons, respectively.

Effect of Pf1 on preformed *C. albicans* biofilm

The results were similar to those for Pf1 activity against biofilm formation. Twofold dilution series then showed 8×10^7 phage ml^{-1} to be the lowest dilution with significant activity. Fig. 4 is representative of seven experiments. This indicates similar activity to that for the Pf4 phage against preformed biofilm, and 10-fold greater activity of Pf1 against preformed biofilm compared to its activity against biofilm formation.

As there are studies indicating that (because of occluding mucus impaction, inflammation and biofilm formation) CF patient airways exist under hypoxic conditions [34–39], we repeated these studies under hypoxic conditions. We saw no differences in the inhibition results when comparing aerobic and hypoxic conditions concurrently, with either phage. Nor did we see differences in phage effects on either Ca biofilm formation or preformed biofilm when comparing aerobic and hypoxic conditions (data not shown).

Phage activity against planktonic *C. albicans* yeasts

Along with testing the impact of Pf phage on Ca biofilms, it was of interest to investigate phage activity against planktonic Ca. This was done using a classical MIC methodology.

When control growth (PBS substituted for phage) was 4+, the only visual reductions of growth occurred at the highest final concentrations (10^{10} phage ml^{-1}) for both Pf4 and Pf1, which were both 2+ (no clear tubes produced at any phage concentration). The results from our assessment of the metabolism, performed using the XTT test on the pelleted cells after incubation with phage, are displayed in Fig. 5 (representative of two experiments; only showing data where the tubes were significantly different from those of the control). Significant alterations in the XTT result were noted with Pf1 down to a 10^9/ml dilution, and with Pf4 to a 10^7 dilution, suggesting 100-fold greater activity of Pf4, although the lower Pf4 dilutions displayed a lesser dose-response curve (before activity was lost at$\leq 10^6$/ml), as had been noted in the biofilm studies. Compared at an identical concentration of 10^{10} phage ml^{-1}, the inhibition by Pf4 was significantly greater than with Pf1.

Iron denial as a mechanism of phage activity

Because of the indication that iron denial was the key mechanism of action of phage against *Aspergillus* [17], we investigated this possibility with phages and *Candida* biofilm formation as well as with preformed biofilm. The results with preformed biofilm for both phages are shown as examples in Figs 6 and 7, which are representative of four experiments. At a *Candida*-inhibiting concentration of 10^{10} Pf4 phage ml^{-1}, Fig. 6 shows, utilizing twofold dilutions of iron,

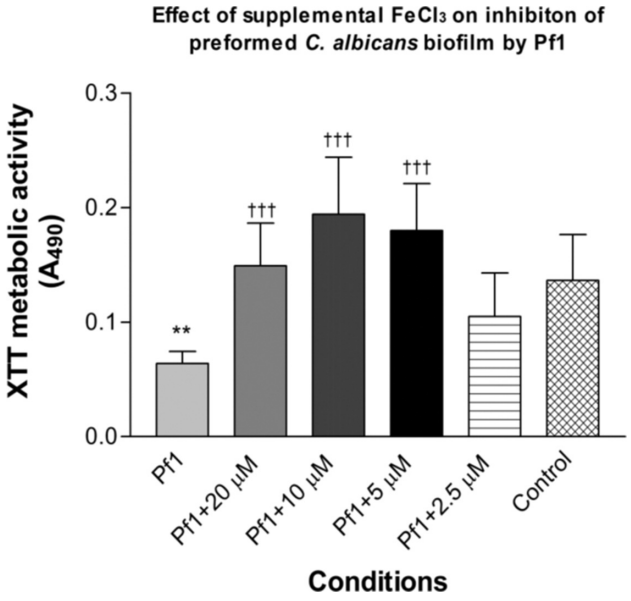

Fig. 7. Reversal by Fe of Pf1 inhibition of preformed *C. albicans* biofilm (XTT assay). 'Control' is no Fe or phage. Pf1 in all other bars was 10^{10} p.f.u. ml^{-1}. Fe at 5–20 μM eliminates the Pf1 inhibition, and at 2.5 μM neutralizes the Pf1 effect. In these experiments Pf1+1.25, 0.625, 0.312, 0.156, 0.078, 0.04, 0.02 or 0.01 μM Fe were also studied (not shown), with those eight combinations not differing from Pf1 alone. Three daggers, $P\leq 0.001$, compared to Pf1 alone. Two asterisks, $P\leq 0.01$ compared to the untreated control.

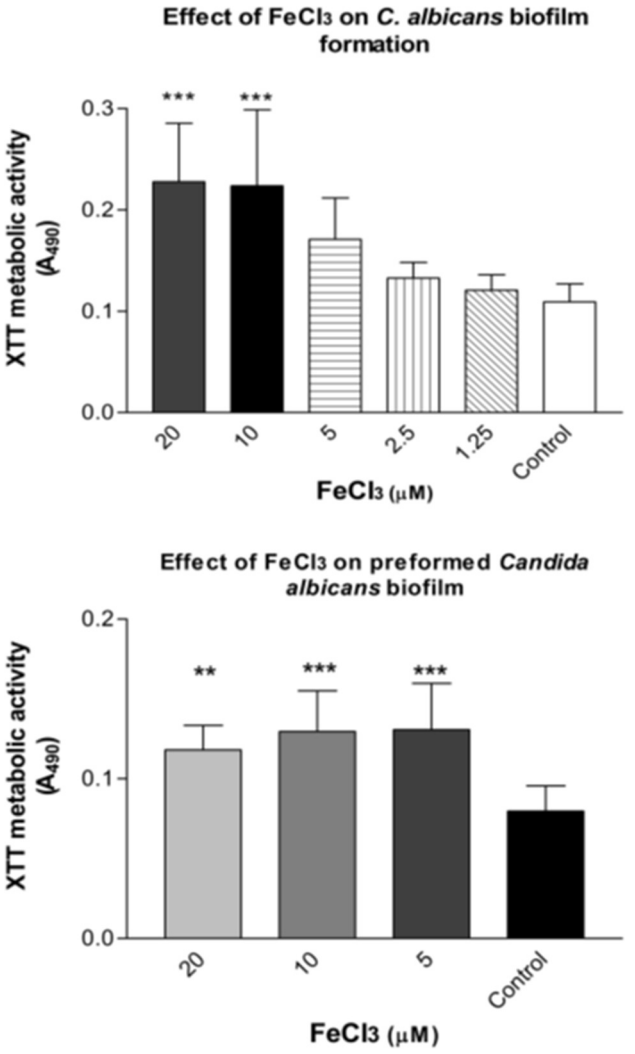

Fig. 8. Stimulation by Fe of *C. albicans*: XTT results. Top: *C. albicans* biofilm formation. 'Control' is no Fe. The *x*-axis shows Fe in μM concentrations. Three asterisks, $P\leq 0.001$, compared to control. Bottom: *C. albicans* preformed biofilm. The arrangement of the bottom panel is the same as for the top. Two and three asterisks indicate $P\leq 0.01$ and $P\leq 0.001$, respectively, compared to untreated control.

that 2.5–20 μM iron eliminates Pf4 inhibition of Ca. However, it is worth noting (Fig. 6) that 2.5 μM iron, an iron concentration that alone does not boost Ca metabolism, neutralizes Pf4 inhibition. In Fig. 7, utilizing a *Candida*-inhibiting concentration of 10^{10} Pf1 phage ml^{-1}, it is noted that, again, 2.5–20 μM iron eliminates Pf1 inhibition. Again, 2.5 μM iron, an iron concentration that does not boost metabolism, neutralizes Pf1 inhibition. The results with the two phages, iron and *Candida* biofilm formation were similar to those shown with preformed biofilm (Figs 6 and 7), and the reversal effect took place over a similar iron concentration, 5–20 μM (data not shown). Not unexpectedly, from prior fungal studies using these assays [32, 40], we find iron alone, at similar concentrations, actually stimulates fungal

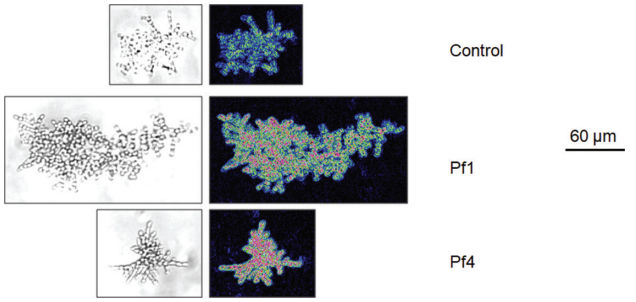

Fig. 9. Birefringence was measured in *C. albicans* biofilms grown in the presence or absence of Pf1 or Pf4 by polarizing microscopy. Duplicate measurements were taken for each biofilm, *n*=5. Ten× objective; left, light microscopy; right, polarizing microscopy.

biofilm metabolism (Fig. 8, representative of four experiments). Evidence of iron boosting fungal metabolism is apparent in Figs 6 and 7 as well.

Birefringence studies of the effect of phages on *Candida* biofilm

At sufficiently high concentrations, filamentous molecular structures, such as inoviruses, spontaneously align [41]. This alignment produces an optical property called birefringence, or double refraction, which can be measured by polarizing microscopy [33]. Recently we reported that Pf phage coating *Aspergillus* increased the birefringence of these biofilms, which was associated with the inhibition of *Aspergillus* metabolism through Pf phage denying iron to *Aspergillus* [17]. Here, we measured the birefringence of Ca biofilms grown in the presence of Pf1 or Pf4. We found that Pf4, and to a lesser extent Pf1, increased the birefringence of *Candida* (Figs 9 and 10), indicating that, as with *Aspergillus* biofilms [17], Pf phages form a highly ordered layer on *Candida* biofilms that alters the polarization of light.

Scanning electron microscopy

Biofilm formation was most notable at the edges of the well chambers, with the centres having sparser growth. Cultures on plastic disks showed enhanced clustered growth, and more compact microcolonies with more pseudohyphae, which were more evenly spread across the substrate than on glass slides. This trend towards denser colonies appeared to be more pronounced in the Pf4-infected cultures (Fig. 11a). Extracellular material was scattered in all cultures (Fig. 11b, arrows). Owing to the absence of surface tension during critical point drying, superficial features were seen best in the preparations made with CPD, and in the phage-infected cultures, particularly Pf4, the observed structures were consistent with phage or phage aggregates in the presence of extracellular matrix (Fig. 11c). The differences between the phage-infected and control cultures under electron microscopy were otherwise not as dramatic as those for the refractometry results (Figs 9 and 10).

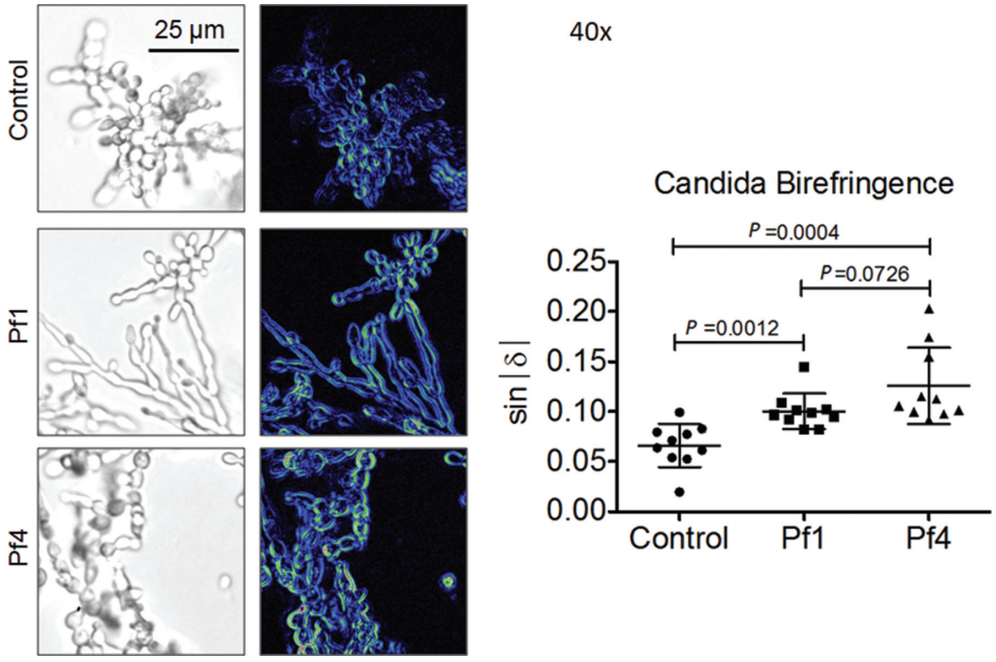

Fig. 10. Birefringence with 40× objective, arrayed as in Fig. 9. The graph compares birefringence measurements between the untreated control, Pf1- and Pf4-treated *Candida* biofilms.

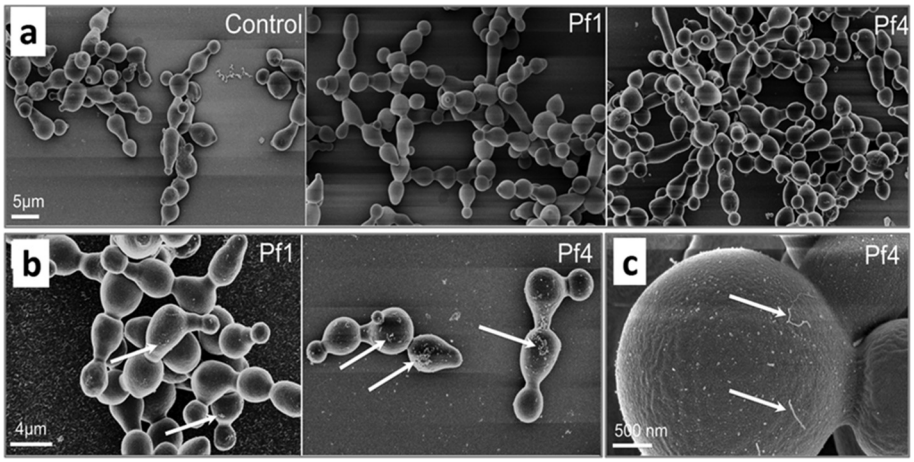

Fig. 11. Scanning electron microscopy views. (a) 5000× magnification. Left, control cultures; centre, Pf1 added; right, Pf4 added. Phages were added at 38 h culture and specimens were prepared at 40 h. Denser colonies were evident in Pf4-infected cultures. (b), 10 000× magnification. Phages were added at 16 h culture, and the specimens were prepared at 40 h. The yeast cells have elongated into pseudohyphal forms, budding has occurred and filamentous forms are seen in other fields. Scattered extracellular material was notable in phage-infected material (arrows) (more prominent in Pf4-infected cultures), which was believed to be altered extracellular matrix materials and/or phage aggregates. (c) Only in Pf4 cultures, and only with the critical-point-drying method (which preserves materials adherent to cells better than HMDS methodology), were the structures observed believed to be phage or phage aggregates (arrows).

DISCUSSION

We have shown an inhibitory effect of bacterial viruses on a fungus, demonstrating that the effects seen on Af [17], a filamentous fungus, also apply to another fungus, one that begins its morphogenetic life as a yeast. Thus this type of interaction may be a more widespread phenomenon in the fungal kingdom. The ability of a bacterial virus to affect the biology of a eukaryote is consistent with other observations we have made with mammalian cells [42].

It will be necessary to study other families of phages with respect to these observations. In the Af studies, the other filamentous phages examined did not show inhibitory power. Intact phage was required [17]. In both the Af and Ca studies, Pf4 effects on fungal metabolism were the endpoints. In the Af studies, direct visual evidence of Pf4 inhibition of growth was also noted; in the present studies this was also suggested with Pf4 in the Ca electron microscopic observations, as mentioned above. Whether these observations concerning inhibition apply to other members of the genus *Candida* is unknown, although preliminary experiments with the phages and *Candida kefyr* (data not shown) indicated the same responses.

The two phages studied here differ substantially in their length; Pf4 is longer than Pf1. It is noteworthy that there were considerable differences between the studies with Af compared to those with Ca. In the Af studies, Pf4 was inhibitory, but Pf1 showed negligible effect. Against Ca, Pf1 was less active against biofilm formation, but showed similar activity to Pf4 against preformed biofilm. Against Af, the Pf4 inhibitory activity was more pronounced against preformed biofilm than biofilm formation, whereas with Ca, the differences were in the opposite direction. Pf1 did not appear to attach to Af biofilm, in contrast to Pf4, whereas the birefringence studies with Ca suggested that Pf1 does bind to Ca, albeit less well than Pf4. The Pf1 binding was notable, in that the electron microscopic studies with the two fungi indicated more physically obvious biofilm formation by Af over the same periods of culture. Another difference between the two sets of studies is the fact that planktonic Af growth appeared to be unaffected by the phages, whereas there was an effect shown on Ca, albeit a small one. Whether the differences in phage potency between the two fungi are related to the attachment differences, or their Fe needs, is presently unknown.

Where the two fungal studies were similar was in the reversal of inhibition by Fe. Moreover, the range of Fe concentrations required to reverse inhibition of both fungi was remarkably similar. Raman studies [17] suggested that Fe and phage crosslink into tight complexes and precipitate out of solution. Although Raman studies [17] indicated that Pf4 binds Fe better than Pf1, the Fe reversal results with the two phages in the present studies were not dissimilar. Whether the binding of phages to biofilm, as suggested by the birefringence and electron microscopic studies, is a necessary part of the posited iron denial (such as by binding to Ca iron-intake mechanisms), or whether phage binding Fe extracellularly is a sufficient competitive event against Ca, is uncertain at this time. These studies focused on Fe, a vital nutrient for Ca [43], Af [44] and Pa [45], and it is competition for Fe that generally seems central to intermicrobial relations [45]. However, we cannot at this point exclude the

possibility that the effects we noted could also similarly involve other cations.

The concentrations of phage demonstrating effects here support possible clinical relevance. Levels of phage in CF patient sputum have been demonstrated to be as high as 10^7/ml [46], and it is likely that phage concentrations will be even higher in the bronchi, such as in the vicinity of packed inspissated endobronchial mucus, debris and microbial biofilms, and when the sample is not diluted (as would occur with sputum) with other uninfected secretions from the whole respiratory tree. Thus, the emerging phage–fungal interactions observed in the laboratory involving Af, and now also Ca, should be considered in models of microbial interaction *in vivo*, and possibly in developing strategies to prevent and eradicate fungal biofilms.

Funding information
Supported in part by a gift from John Flatley to the California Institute for Medical Research (#3770) (D. A. S., H. N. and G. S.) and National Science Foundation CAREER award 1453247 (to L. C.). The funders were not involved in the study, the preparation of the article, or the decision to publish.

Conflicts of interest
The authors declare that there are no conflicts of interest.

References

1. Williams HD, Davies JC. Basic science for the chest physician: *Pseudomonas aeruginosa* and the cystic fibrosis airway. *Thorax* 2012;67:465–467.
2. Bhargava V, Tomashefski JF, Stern RC, Abramowsky CR. The pathology of fungal infection and colonization in patients with cystic fibrosis. *Hum Pathol* 1989;20:977–986.
3. Cimon B, Carrere J, Chazalette JP, Ginies JL, Six P *et al.* Fungal colonization and immune response to fungi in cystic fibrosis. *J Mycol Med* 1995;5:211–216.
4. Nagano Y, Millar BC, Johnson E, Goldsmith CE, Elborn JS *et al.* Fungal infections in patients with cystic fibrosis. *Rev Med Microbiol* 2007;18:11–16.
5. Horré R, Symoens F, Delhaes L, Bouchara JP. Fungal respiratory infections in cystic fibrosis: a growing problem. *Med Mycol* 2010; 48:S1–S3.
6. Middleton PG, Chen SC, Meyer W. Fungal infections and treatment in cystic fibrosis. *Curr Opin Pulm Med* 2013;19:670–675.
7. Anand R, Moss RB, Sass G, Banaei N, Clemons KV *et al.* Small colony variants of *Pseudomonas aeruginosa* display heterogeneity in inhibiting *Aspergillus fumigatus* biofilm. *Mycopathologia* 2017 (In press).
8. Hogan DA, Kolter R. *Pseudomonas-Candida* interactions: an ecological role for virulence factors. *Science* 2002;296:2229–2232.
9. Hogan DA, Vik A, Kolter R. A *Pseudomonas aeruginosa* quorum-sensing molecule influences *Candida albicans* morphology. *Mol Microbiol* 2004;54:1212–1223.
10. Holcombe LJ, Mcalester G, Munro CA, Enjalbert B, Brown AJ *et al.* *Pseudomonas aeruginosa* secreted factors impair biofilm development in *Candida albicans*. *Microbiology* 2010;156:1476–1486.
11. Hall RA, Turner KJ, Chaloupka J, Cottier F, de Sordi L *et al.* The quorum-sensing molecules farnesol/homoserine lactone and dodecanol operate via distinct modes of action in *Candida albicans*. *Eukaryot Cell* 2011;10:1034–1042.
12. Bandara HM, K Cheung BP, Watt RM, Jin LJ, Samaranayake LP. *Pseudomonas aeruginosa* lipopolysaccharide inhibits *Candida albicans* hyphae formation and alters gene expression during biofilm development. *Mol Oral Microbiol* 2013;28:54–69.
13. Singh N, Pemmaraju SC, Pruthi PA, Cameotra SS, Pruthi V. Candida biofilm disrupting ability of di-rhamnolipid (RL-2) produced from *Pseudomonas aeruginosa* DSVP20. *Appl Biochem Biotechnol* 2013;169:2374–2391.
14. Tupe SG, Kulkarni RR, Shirazi F, Sant DG, Joshi SP *et al.* Possible mechanism of antifungal phenazine-1-carboxamide from *Pseudomonas* sp. against dimorphic fungi *Benjaminiella poitrasii* and human pathogen *Candida albicans*. *J Appl Microbiol* 2015; 118:39–48.
15. Lopez-Medina E, Fan D, Coughlin LA, Ho EX, Lamont IL *et al.* *Candida albicans* Inhibits *Pseudomonas aeruginosa* virulence through suppression of pyochelin and pyoverdine biosynthesis. *PLoS Pathog* 2015;11:e1005129.
16. Secor PR, Sweere JM, Michaels LA, Malkovskiy AV, Lazzareschi D *et al.* Filamentous bacteriophage promote biofilm assembly and function. *Cell Host Microbe* 2015;18:549–559.
17. Penner JC, Ferreira JA, Secor PR, Sweere JM, Birukova MK *et al.* Pf4 bacteriophage produced by *Pseudomonas aeruginosa* inhibits *Aspergillus fumigatus* metabolism via iron sequestration. *Microbiology* 2016;162:1583–1594.
18. Noni M, Katelari A, Kaditis A, Theochari I, Lympari I *et al.* *Candida albicans* chronic colonisation in cystic fibrosis may be associated with inhaled antibiotics. *Mycoses* 2015;58:416–421.
19. Chotirmall SH, O'Donoghue E, Bennett K, Gunaratnam C, O'Neill SJ *et al.* Sputum *Candida albicans* presages FEV_1 decline and hospital-treated exacerbations in cystic fibrosis. *Chest* 2010;138: 1186–1195.
20. Gileles-Hillel A, Shoseyov D, Polacheck I, Korem M, Kerem E *et al.* Association of chronic *Candida albicans* respiratory infection with a more severe lung disease in patients with cystic fibrosis. *Pediatr Pulmonol* 2015;50:1082–1089.
21. Liu M, Clemons KV, Johansen ME, Martinez M, Chen V *et al.* Saccharomyces as a vaccine against systemic candidiasis. *Immunol Invest* 2012;41:847–855.
22. Ramage G, Vandewalle K, Bachmann SP, Wickes BL, López-Ribot JL. *In vitro* pharmacodynamic properties of three antifungal agents against preformed *Candida albicans* biofilms determined by time-kill studies. *Antimicrob Agents Chemother* 2002;46:3634–3636.
23. Li X, Yan Z, Xu J. Quantitative variation of biofilms among strains in natural populations of *Candida albicans*. *Microbiology* 2003;149: 353–362.
24. Kuhn DM, Balkis M, Chandra J, Mukherjee PK, Ghannoum MA. Uses and limitations of the XTT assay in studies of Candida growth and metabolism. *J Clin Microbiol* 2003;41:506–508.
25. Chandra J, Mukherjee PK, Ghannoum MA. *In vitro* growth and analysis of *Candida* biofilms. *Nat Protoc* 2008;3:1909–1924.
26. Pierce CG, Uppuluri P, Tristan AR, Wormley FL, Mowat E *et al.* A simple and reproducible 96-well plate-based method for the formation of fungal biofilms and its application to antifungal susceptibility testing. *Nat Protoc* 2008;3:1494–1500.
27. Jacobs MA, Alwood A, Thaipisuttikul I, Spencer D, Haugen E *et al.* Comprehensive transposon mutant library of *Pseudomonas aeruginosa*. *Proc Natl Acad Sci USA* 2003;100:14339–14344.
28. Boulanger P. Purification of bacteriophages and SDS-PAGE analysis of phage structural proteins from ghost particles. *Methods Mol Biol* 2009;502:227-38.
29. Hmelo LR, Borlee BR, Almblad H, Love ME, Randall TE *et al.* Precision-engineering the *Pseudomonas aeruginosa* genome with two-step allelic exchange. *Nat Protoc* 2015;10:1820–1841.
30. Castang S, Dove SL. Basis for the essentiality of H-NS family members in *Pseudomonas aeruginosa*. *J Bacteriol* 2012;194:5101–5109.

31. **Anand R, Clemons KV, Stevens DA.** Effect of anaerobiasis or hypoxia on *Pseudomonas aeruginosa* Inhibition of *Aspergillus fumigatus* Biofilm. *Arch Microbiol* 2017;199:881–890.
32. **Ferreira JA, Penner JC, Moss RB, Haagensen JA, Clemons KV *et al.*** Inhibition of *Aspergillus fumigatus* and its biofilm by *Pseudomonas aeruginosa* is dependent on the source, phenotype and growth conditions of the bacterium. *PLoS One* 2015;10:e0134692.
33. **Glazer AM, Lewis JG, Kaminsky W.** An automatic optical imaging system for birefringent media. *Proc R Soc Lond A* 1996;452:2751–2765.
34. **Costerton JW.** Anaerobic biofilm infections in cystic fibrosis. *Mol Cell* 2002;10:699–700.
35. **Yoon SS, Hennigan RF, Hilliard GM, Ochsner UA, Parvatiyar K *et al.*** *Pseudomonas aeruginosa* anaerobic respiration in biofilms: relationships to cystic fibrosis pathogenesis. *Dev Cell* 2002;3:593–603.
36. **Worlitzsch D, Tarran R, Ulrich M, Schwab U, Cekici A *et al.*** Effects of reduced mucus oxygen concentration in airway *Pseudomonas* infections of cystic fibrosis patients. *J Clin Invest* 2002;109:317–325.
37. **Werner E, Roe F, Bugnicourt A, Franklin MJ, Heydorn A *et al.*** Stratified growth in *Pseudomonas aeruginosa* biofilms. *Appl Environ Microbiol* 2004;70:6188–6196.
38. **Lambiase A, Catania MR, Rossano F.** Anaerobic bacteria infection in cystic fibrosis airway disease. *New Microbiol* 2010;33:185–194.
39. **Cowley ES, Kopf SH, Lariviere A, Ziebis W, Newman DK.** Pediatric cystic fibrosis sputum can be chemically dynamic, anoxic, and extremely reduced due to hydrogen sulfide formation. *MBio* 2015; 6:e00767.
40. **Nazik H, Penner JC, Ferreira JA, Haagensen JA, Cohen K *et al.*** Effects of iron chelators on the formation and development of *Aspergillus fumigatus* biofilm. *Antimicrob Agents Chemother* 2015; 59:6514–6520.
41. **Dogic Z, Fraden S.** Ordered phases of filamentous viruses. *Curr Opin Colloid Interface Sci* 2006;11:47–55.
42. **Secor PR, Michaels LA, Smigiel KS, Rohani MG, Jennings LK *et al.*** Filamentous bacteriophage produced by *Pseudomonas aeruginosa* alters the inflammatory response and promotes noninvasive infection *in vivo*. *Infect Immun* 2017;85:e00648-16.
43. **Noble SM.** *Candida albicans* specializations for iron homeostasis: from commensalism to virulence. *Curr Opin Microbiol* 2013;16: 708–715.
44. **Schrettl M, Haas H.** Iron homeostasis—Achilles' heel of *Aspergillus fumigatus*? *Curr Opin Microbiol* 2011;14:400–405.
45. **Nguyen AT, Oglesby-Sherrouse AG.** Spoils of war: iron at the crux of clinical and ecological fitness of *Pseudomonas aeruginosa*. *Biometals* 2015;28:433–443.
46. **Tejedor C, Foulds J, Zasloff M.** Bacteriophages in sputum of patients with bronchopulmonary *Pseudomonas* infections. *Infect Immun* 1982;36440–441.

Edited by: A. Alastruey-Izquierdo and V. J. Cid